Electronic Supplementary Information

Redox-Driven Strong Interfacial Interactions between MnO_2 and Covalent Organic Nanosheets for Efficient Oxygen Reduction Electrocatalysis

Min-Sung Kim,[‡,a] Tae-Ha Gu,[‡,b] Soohyeon Park,[‡,a] Taehoon Kim,[b] Yun Kyung Jo,[c] Young Kyu Jeong,[,d] Jin Kuen Park[*,a] and Seong-Ju Hwang[*,b]*

M.-S. Kim, S. Park, Prof. J. K. Park
[a] Department of Chemistry, Hankuk University of Foreign Studies, Yongin, 449-791, Gyeonggi-do, Republic of Korea
E-mail: jinkpark@hufs.ac.kr

Dr. T. H. Gu, T. Kim, Prof. S.-J. Hwang
[b] Department of Materials Science and Engineering, Yonsei University, Seoul 03722, Republic of Korea
E-mail: hwangsju@yonsei.ac.kr

Dr. Y. K. Jo
[c] Department of Chemistry and Nanosciences, Ewha Womans University, Seoul 03760, Republic of Korea

Dr. Y. K. Jeong (Ph.D.)
[d] Korea Institute of Industrial Technology, 137-41 Gwahakdanji-ro, Gangneung-si, Gangwon 25440, Republic of Korea
E-mail: immrc80@gmail.com

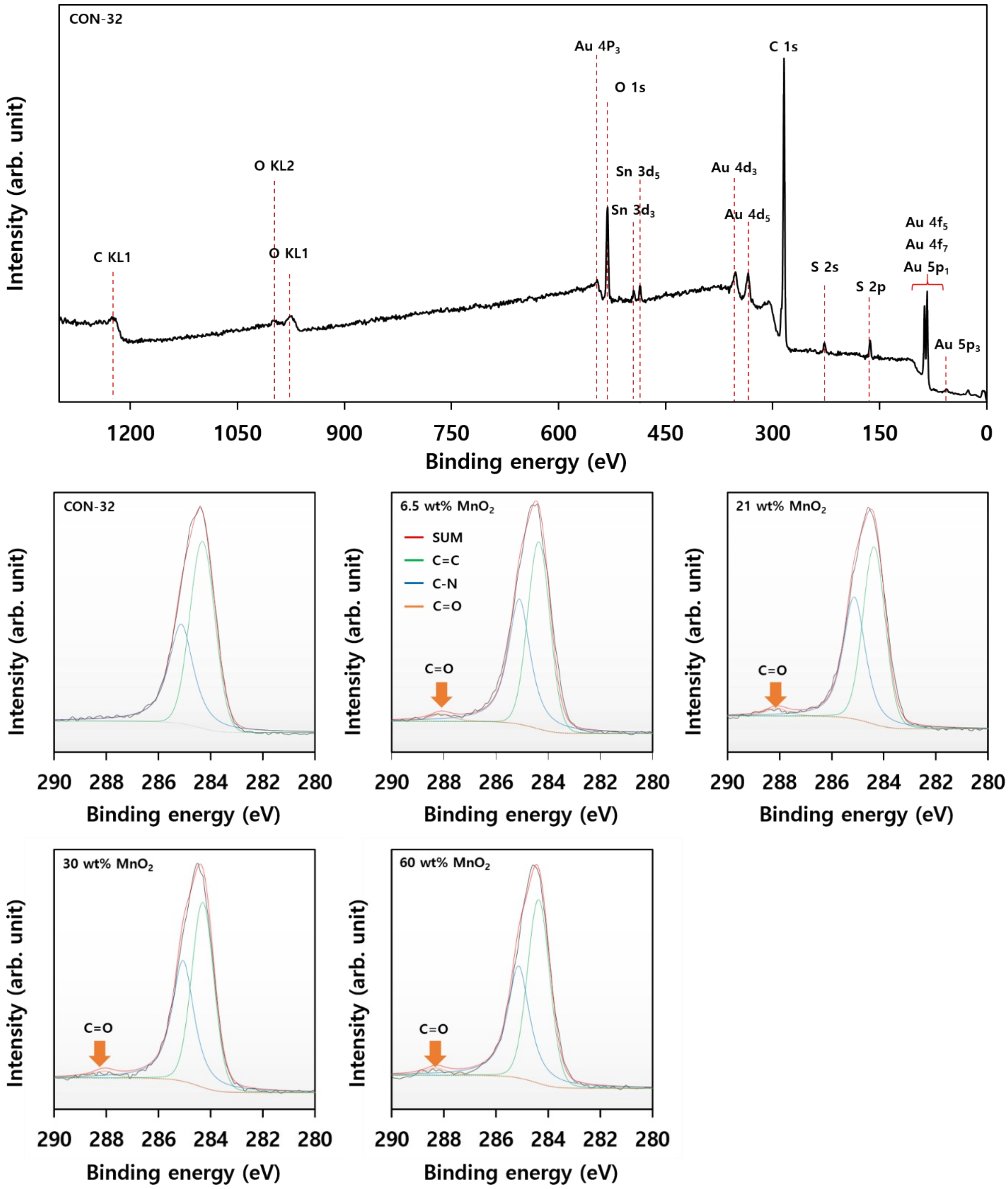

Figure S1. XPS full profiles of CON-32 and carbon spectrum of the pristine CON-32 and various hybrid materials with varying MnO_2 wt% when they were synthesized, then after purified with Soxhlet extraction.

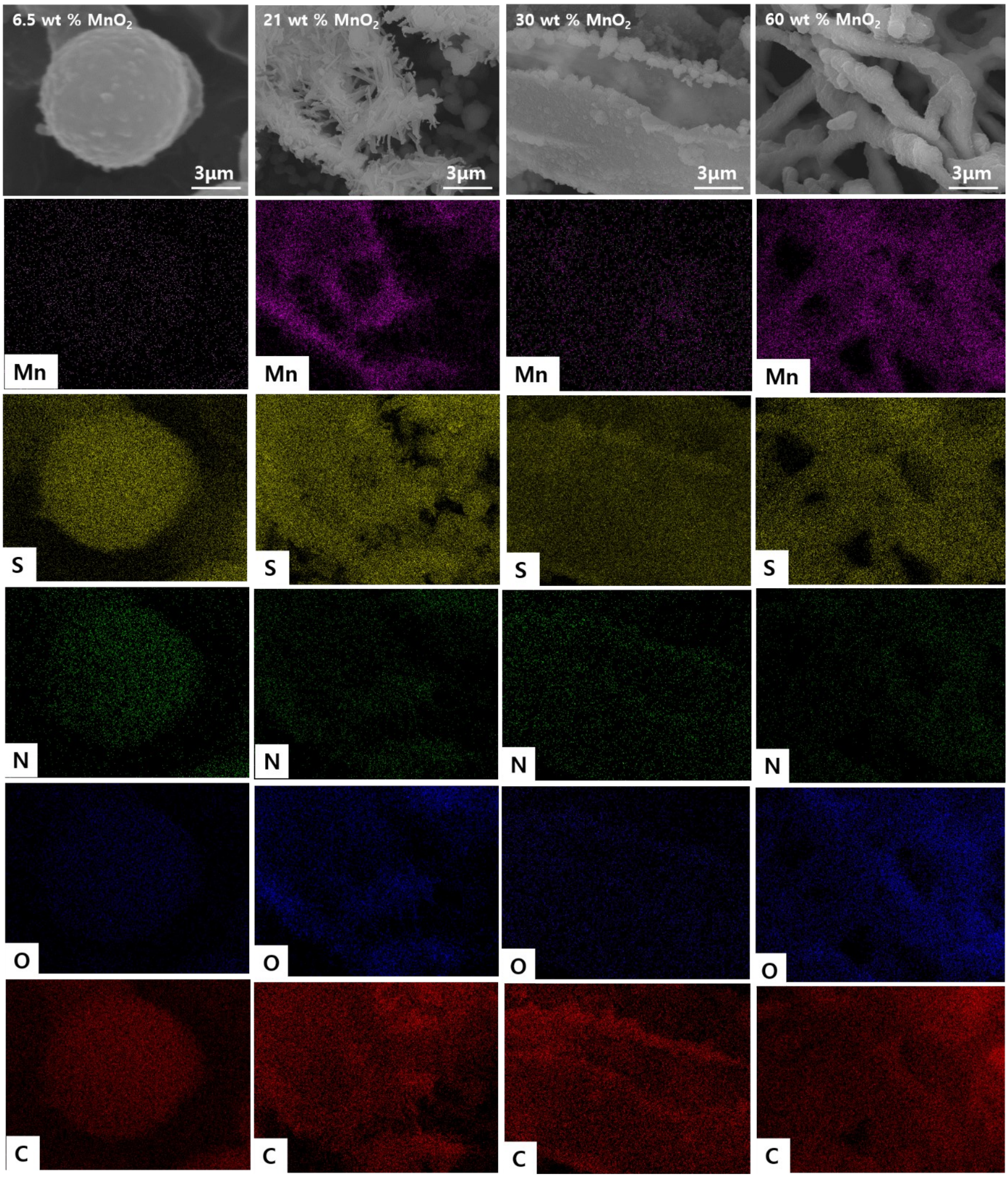

Figure S2. The magnified scanning electron microscopy (SEM) images of hybrids with varying MnO_2 contents together with their energy dispersive x-ray spectroscopy (EDS)–elemental mapping at the same spots of SEM images with respect to S, N, O, C and Mn.

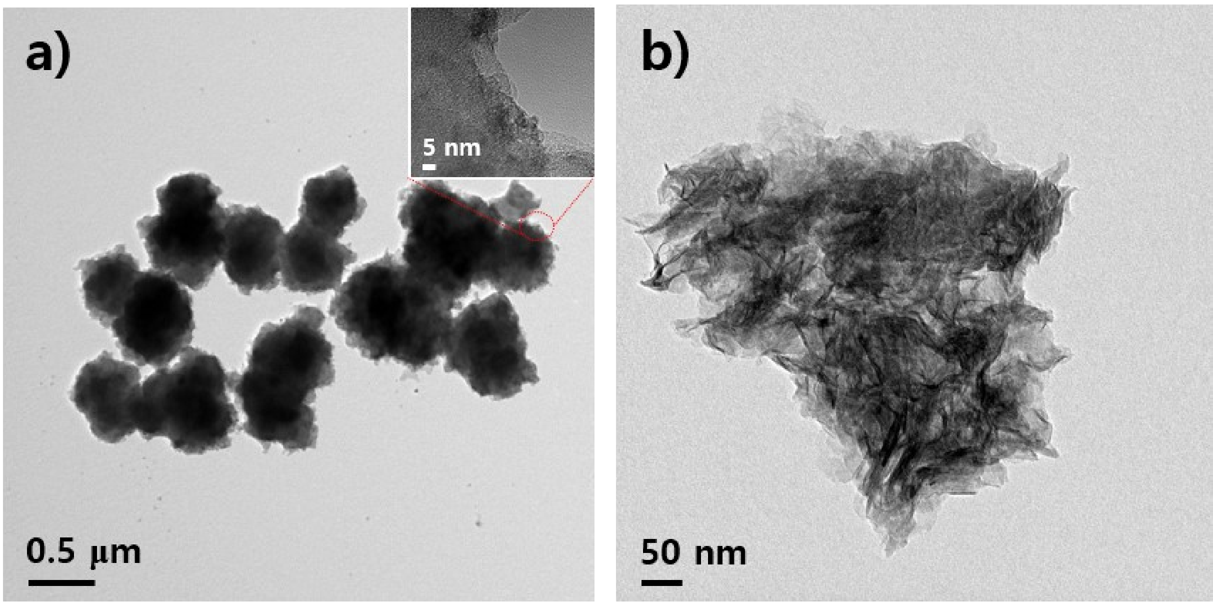

Figure S3. The transmission electron microscopy (TEM) images of (a) pristine CON-32 and (b) pristine exfoliated layered MnO_2.

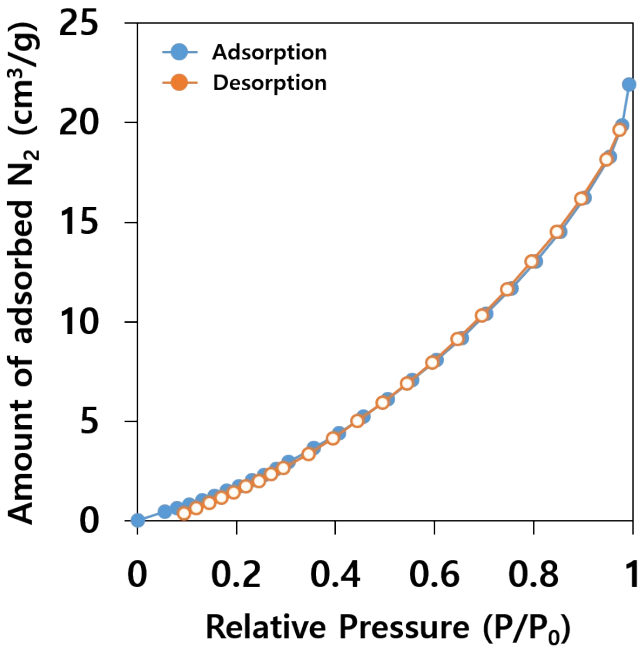

Figure S4. The N_2 adsorption/desorption isotherm profiles of pristine layered MnO_2.

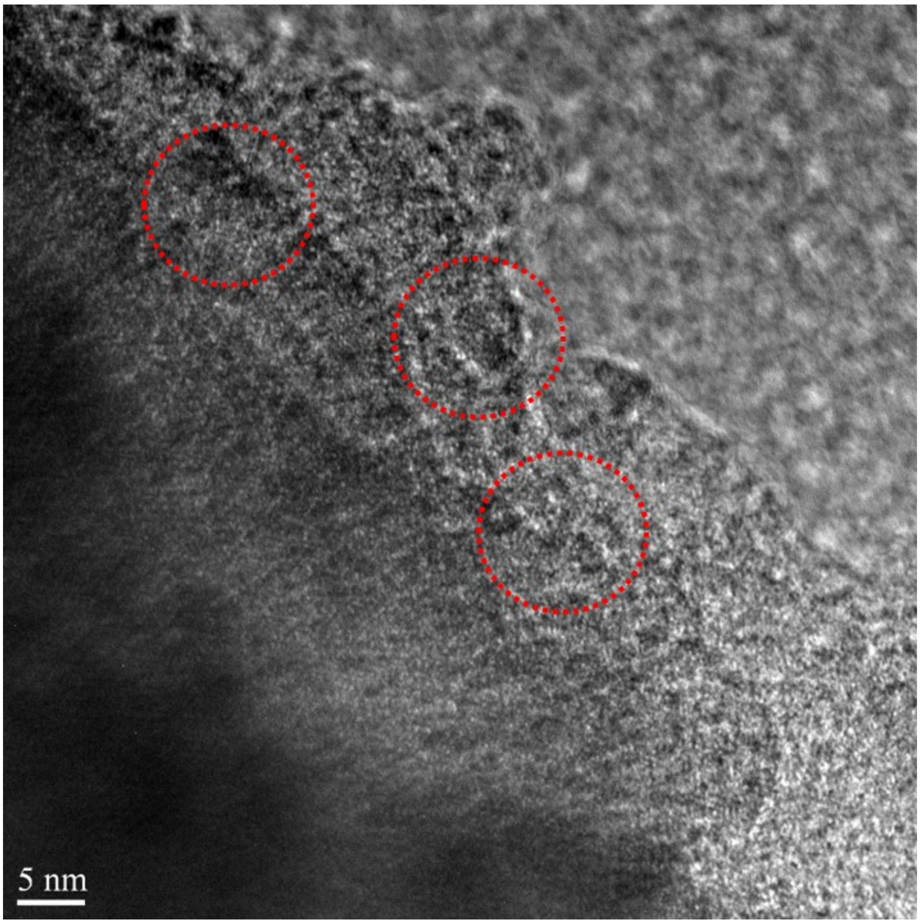

Figure S5. The TEM images of pristine CON-32.

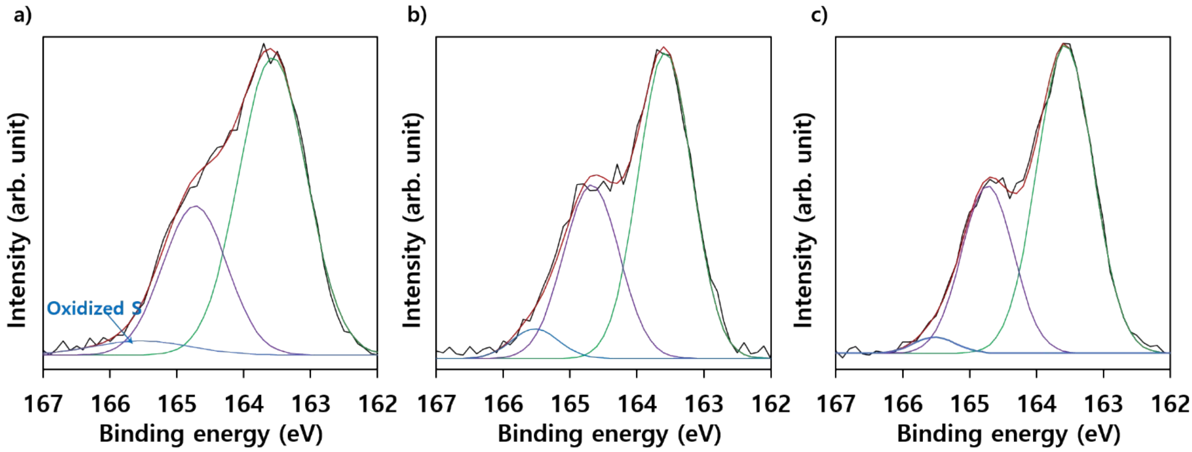

Figure S6. The XPS profiles of hybrids with (a) 6.5 wt% MnO_2, (b) 30 wt% MnO_2 and (c) 60 wt% MnO_2, after purified by Soxhlet extraction respectively.

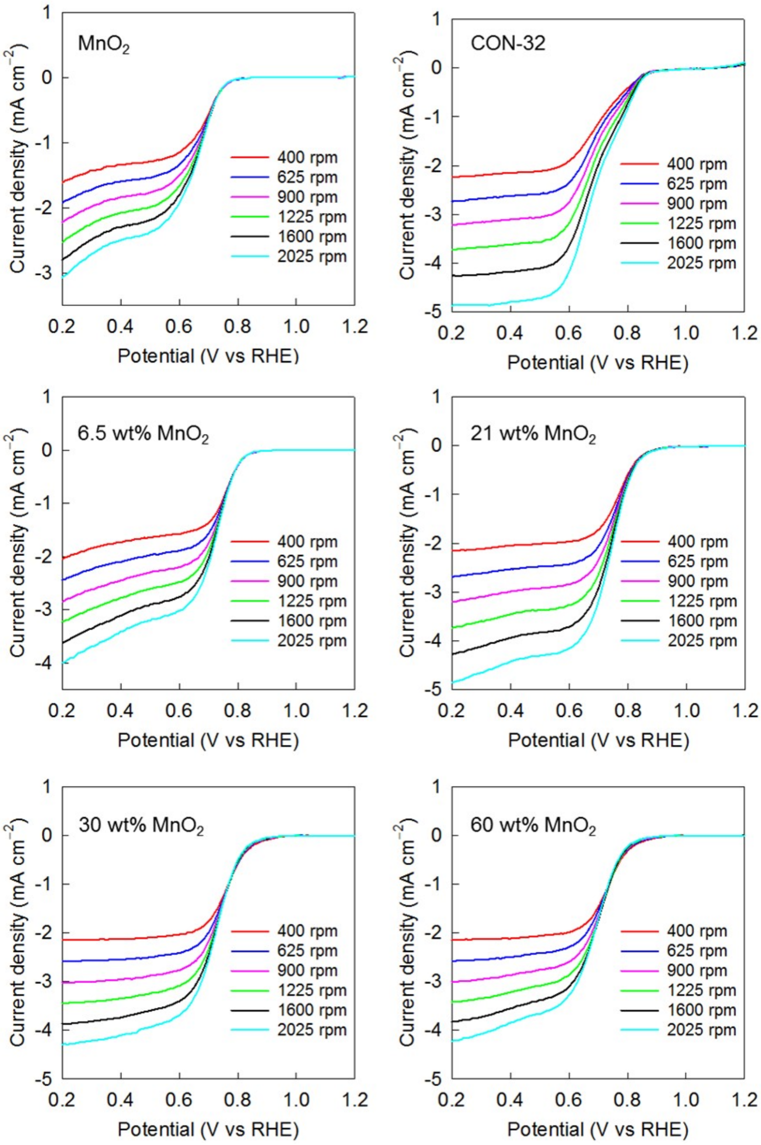

Figure S7. Linear sweep voltammetry (LSV) profiles of precursors MnO_2, CON, as-prepared hybrids with 6.5 wt%, 21 wt%, 30 wt% and 60 wt% MnO_2 with the rotation rates of 400–2025 rpm.

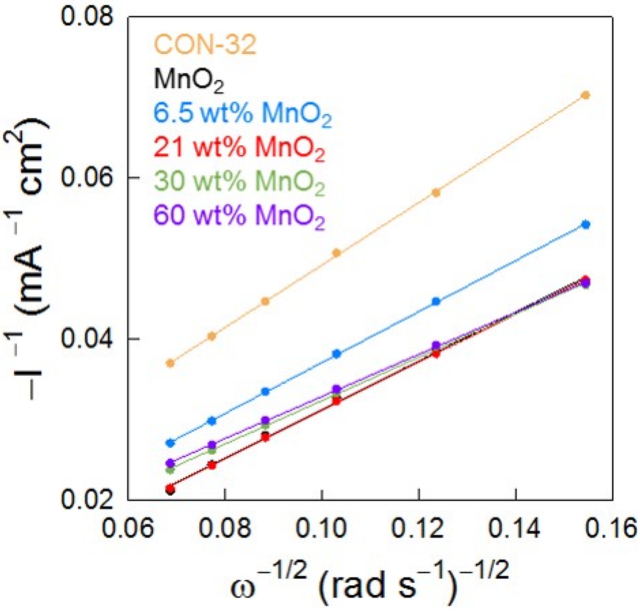

Figure S8. Koutecky–Levich (K–L) profiles of precursors MnO_2, CON, as-prepared hybrids with 6.5 wt%, 21 wt%, 30 wt% and 60 wt% MnO_2.

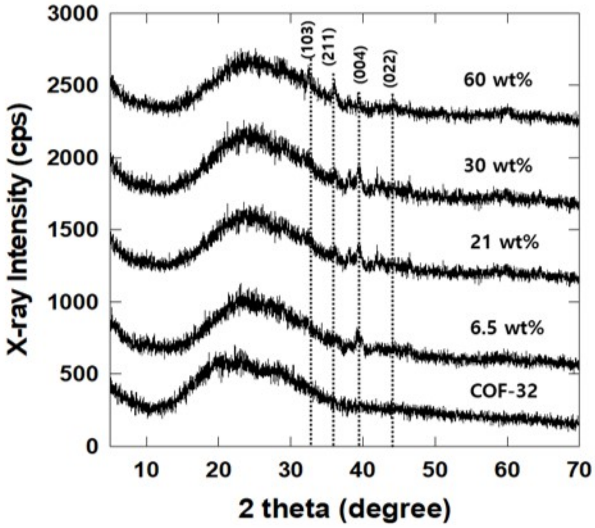

Figure S9. Powder x-ray diffraction (PXRD) patterns of carbonized CON-32 and carbonized hybrids with varying MnO_2 contents at 800 °C under Ar atmosphere; the PXRD peak indexes represent some specific Mn_3O_4 phases.

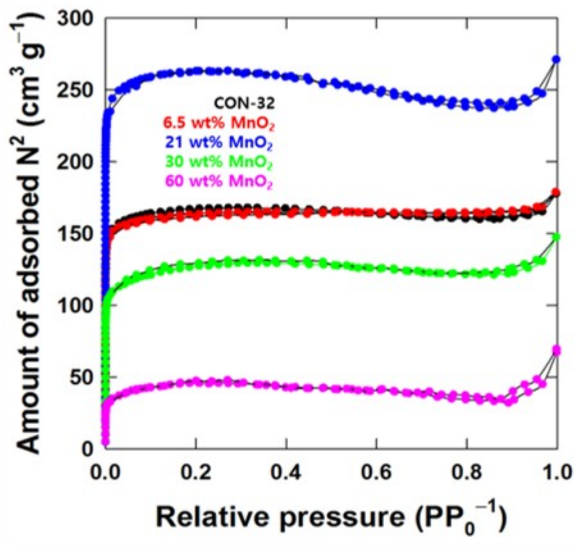

Figure S10. N_2 adsorption/desorption isotherm profiles of carbonized CON-32 and carbonized hybrids with varying MnO_2 contents at 800 °C under Ar atmosphere.

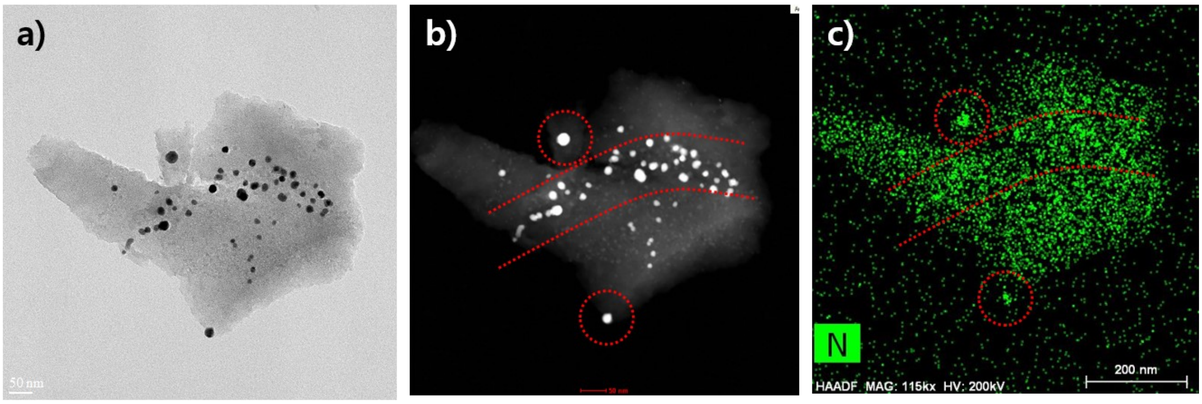

Figure S11. (a) TEM images of carbonized hybrid with 6.5 wt% MnO_2; together with (b) scanning transmission electron microscopy (STEM) images and (c) EDS–elemental mapping of N at the same spots of TEM and STEM images.

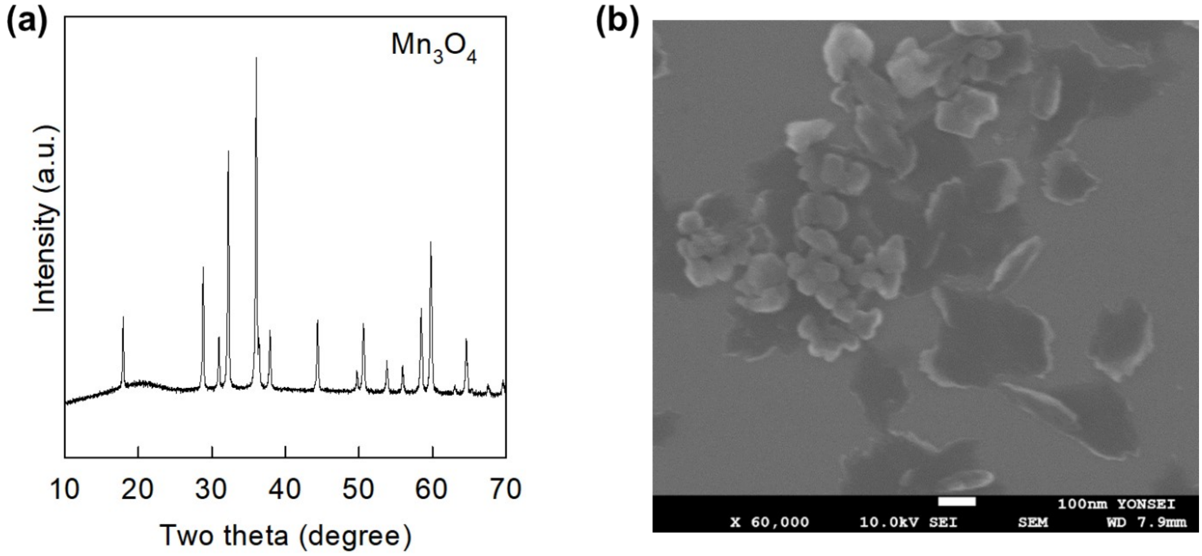

Figure S12. (a) PXRD pattern and (b) FE-SEM image of Mn_3O_4 prepared by the heat-treatment of MnO_2 nanosheet at 800 °C in Ar atmosphere.

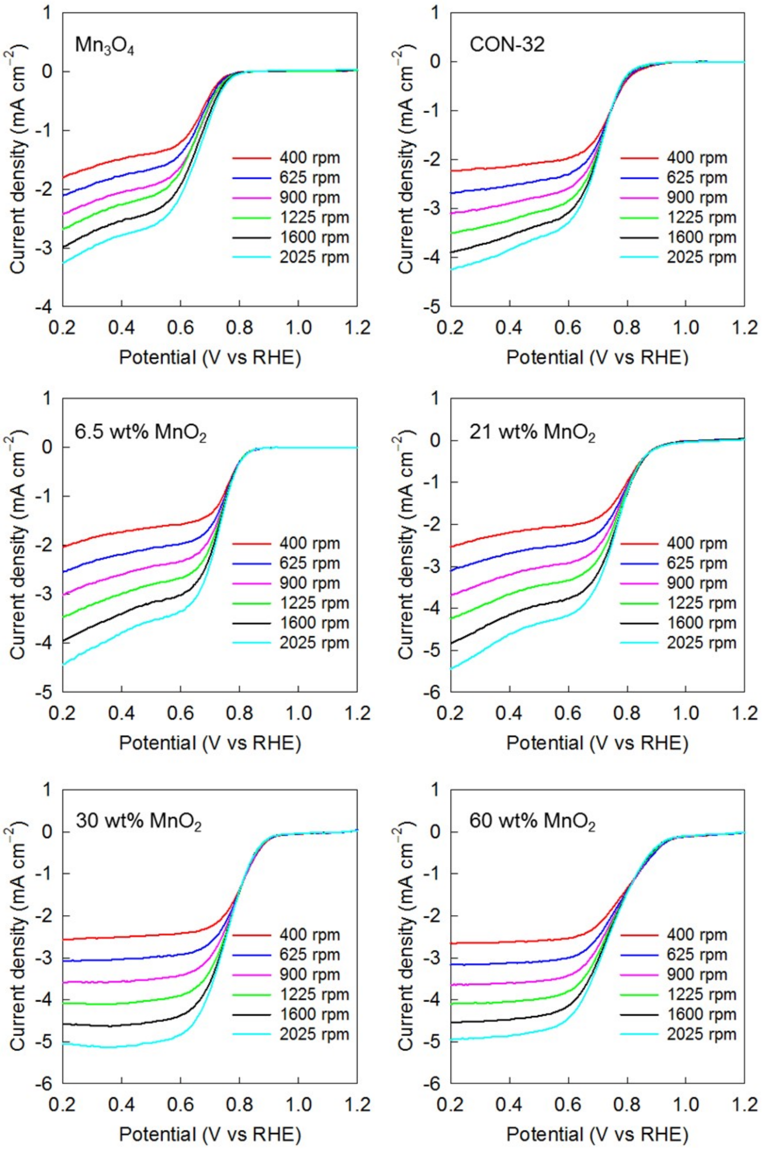

Figure S13. LSV profiles of carbonated CON, Mn_3O_4, carbonized hybrids at 800 °C with 6.5 wt% MnO_2, 21 wt% MnO_2, 30 wt% MnO_2 and 60 wt% MnO_2 with the rotation rates of 400−2025 rpm.

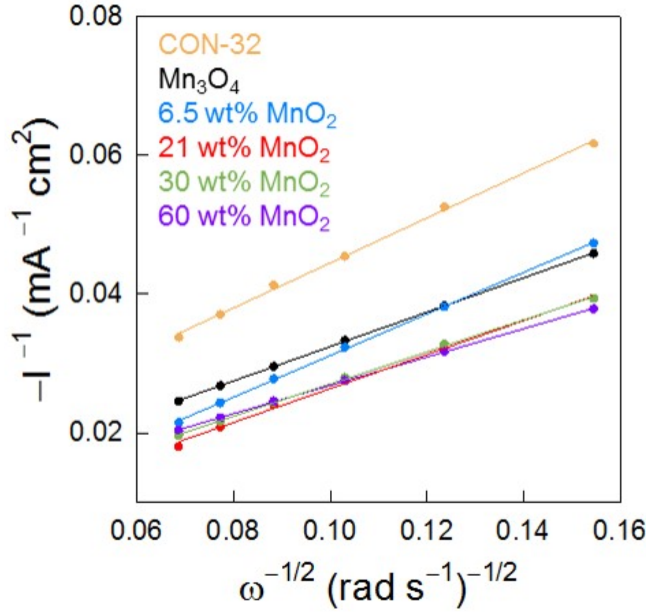

Figure S14. K−L profiles of carbonated CON, Mn_3O_4, carbonized hybrids at 800 °C with 6.5 wt% MnO_2, 21 wt% MnO_2, 30 wt% MnO_2 and 60 wt% MnO_2.

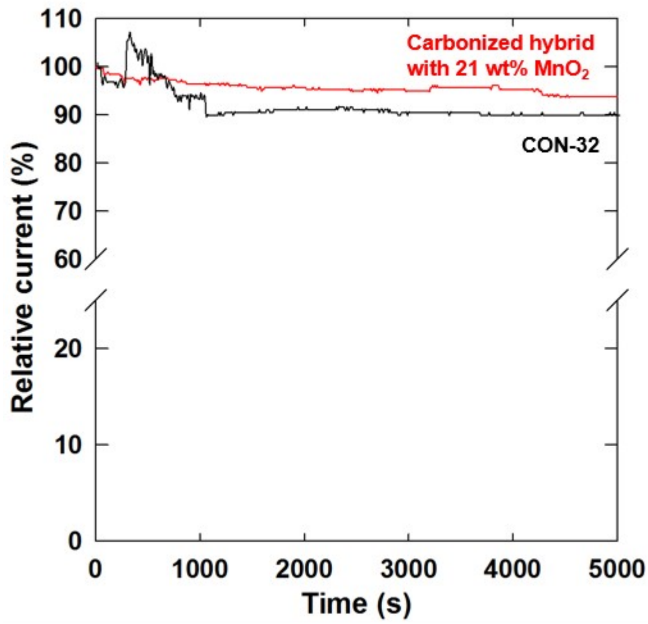

Figure S15. The long term stabilities of carbonized CON-32 and carbonized hybrid with 21 wt% MnO_2 at 800 °C under Ar atmosphere.

Table S1. Charge transfer resistance (R_{ct}) values of precursors MnO_2, CON, as-prepared hybrids with 6.5 wt%, 21 wt%, 30 wt% and 60 wt% MnO_2.

Material	**R_{ct} (Ω)**
CON-32	436.5
MnO_2	261.4
6.5 wt% MnO_2	152.5
21 wt% MnO_2	132.7
30 wt% MnO_2	180.5
60 wt% MnO_2	199.1

Table S2. Comparison of ORR electrocatalytic performance of COF based catalysts in 0.1 M KOH.

Material	$E_{1/2}$ (V vs RHE)	Tafel slope (mV dec^{-1})	n	Ref
21wt% MnO_2	0.79	64	3.48	This work
COF@MOF_{800}-Fe	0.89	80	3.97	1
Pt-COF@MOF_{800}	0.85	21	3.94	2
Ni/Fe-COF@CNT_{900}	0.87	61	3.95	3
LTHT-FeP	0.83	-	-	4
JUC-528	0.70	65.9	3.81	5
Fe_{AC}@Fe_{SA}-N-C	0.912	61	3.9	6
mC-TpBpy-Fe	0.845	-	~4	7
$Fe_{0.5}Co_{0.5}$Pc-CP NS@G	0.927	-	3.9	8
PTEBbpyCu4.5-HT	0.72 (900 rpm)	-	3.95	9
1”-NP	0.81	70	~4	10
FeNi-COP-800	0.803	91	3.9	11

Table S3. R_{ct} values of carbonated CON, Mn_3O_4, carbonized hybrids at 800 °C with 6.5 wt% MnO_2, 21 wt% MnO_2, 30 wt% MnO_2 and 60 wt% MnO_2.

Material	**R_{ct} (Ω)**
CON-32	286.7
Mn_3O_4	218.1
6.5 wt% MnO_2	117.1
21 wt% MnO_2	96.2
30 wt% MnO_2	143.8
60 wt% MnO_2	162.8

Reference

1. Q. Miao, S. Yang, Q. Xu, M. Liu, P. Wu, G. Liu, C. Yu, Z. Jiang, Y. Sun and G. Zeng, *Small Struct.*, 2022, **3**, 2100225.
2. Y. Guo, S. Yang, Q. Xu, P. Wu, Z. Jiang and G. Zeng, *J. Mater. Chem. A.*, 2021, **9**, 23625−13630.
3. Q. Xu, J. Qian, D. Luo, G. Liu, Y. Guo and G. Zeng, *Adv. Sustain. Syst.*, 2020, **4**, 2000115.
4. N. Zion, D. A. Cullen, P. Zelenay and L. Elbaz, *Angew. Chem. Int. Ed.,* 2019, **59**, 2483–2489.
5. D. Li, C. Li, L. Zhang, H. Li, L. Zhu, D. Yang, Q. Fang, S. Qiu and X. Yao, *J. Am. Chem. Soc.*, 2020, **142**, 8104–8108.
6. X. Ao, W. Zhang, Z. Li, J. G. Li, L. Soule, X. Huang, W. H. Chiang, H. M. Chen, C. Wang, M. Liu and X. C. Zeng, *ACS Nano,* 2019, **13**, 11853−11862.
7. X. Zhao, P. Pachfule, S. Li, T. Langenhahn, M. Ye, G. Tian, J. Schmidt and A. Thomas, *Chem. Mater.,* 2019, **31**, 3274–3280.
8. W. Liu, C. Wang, L. Zhang, H. Pan, W. Liu, J. Chen, D. Yang, Y. Xiang, K. Wang, J. Jiang and X. Yao, *J. Am. Chem. Soc.,* 2019, **7**, 3112–3119.
9. L. P. Strahl, N. Zion, O. Lori, N. Levy, G. Bar, A. Dahan and L. Elbaz, *Adv. Funct. Mater.,* 2021, **31**, 2100163.
10. C. Yang, S. Tao, N. Huang, X. Zhang, J. Duan, R. Makiura and S. Maenosono, *ACS Appl. Nano. Mater.*, 2020, **3**, 5481−5488.
11. Z. Liao, Y. Wang, Q. Wang, Y. Cheng and Z. Xiang, *Appl. Catal. B-Environ.*, 2019, **243**, 204–211.